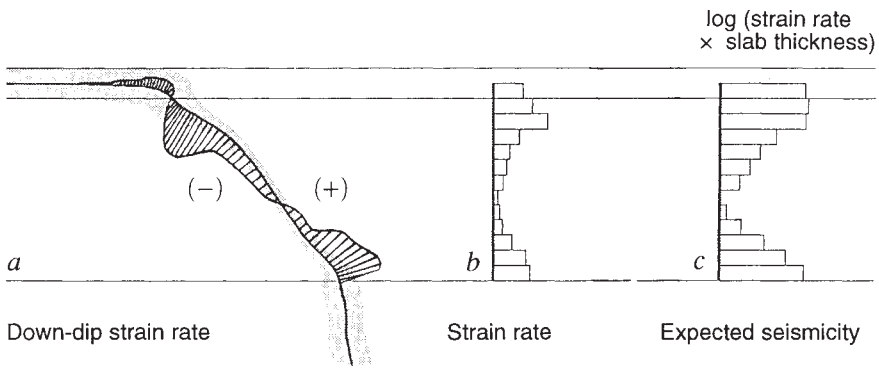

FIG. 4 Strain rates and expected rates of seismicity in a fluid slab. *a*, Strain rate within slab of Fig. 3*b* (mantle viscosity increases by factor of 10 at 670 km). Strain rate is plotted using centre of slab as axis; curve to the right of the axis indicates compression (+), to the left indicates extension (−). Minimal deformation occurs midslab at the crossover from extension to compression, and the most vigorous strain rates occur as the slab draws away from the surface and as it nears the viscosity step at 670 km. The areas of maximal strain rate coincide with the regions of greatest slab thickness. Below 670 km, down-dip strain rates drop precipitously. *b*, Integral of strain rates (integrated down-dip) at 50-km depth intervals. *c*, Logarithm of expected seismicity, calculated by taking the integral of the down-dip strain rate multiplied by slab thickness. In the weak-slab model, the number of earthquakes peaks where strain rates and slab thickness are greatest. The resulting curve resembles that of Fig. 1: there is an exponential decay with depth from the surface to the midslab, corresponding to a region of downdip extension, followed by a compressional resurgence at depth. Below 670 km, the abrupt drop in strain rate may allow the slab to sink aseismically.

From the deformation history of our experimental slabs, we calculate the expected variation of seismicity with depth (Fig. 4). We assume that all parts of the lithosphere are firmly bound together and hence deform at equal rates. Whether earthquakes are distributed throughout a slab or are concentrated in a seismogenic layer, the number of earthquakes within a given depth interval will be proportional to the amount of slab material present and to the rate of down-dip strain.

In Fig. 4*a* we plot the instantaneous strain rate for the slab in Fig. 3*b*. Extensional and compressional peaks are seen towards the top and bottom of the slab, with a decrease in strain rate in the cross-over region in between and an abrupt drop in strain rate beneath 670 km. Integrating this strain rate along the slab over successive depth intervals gives Fig. 4*b*. To obtain the expected seismicity, we must take into account the thickness of the slab (and hence of the seismogenic region) at different depths. We therefore multiply the integrated strain rate by slab thickness to obtain the expected seismicity distribution in Fig. 4*c*.

Given the extreme simplicity of the experimental model, the calculated seismicity pattern (Fig. 4*c*) is remarkably similar to that observed (Fig. 1). In both, the rate of seismicity decreases exponentially with depth in the upper slab, achieves a minimum at intermediate depths and increases towards 670 km in a region of down-dip compression. Moreover, our results suggest a simple mechanism for aseismic slab penetration into the lower mantle: if mantle viscosity increases moderately at 670 km, slab strain rates abruptly decrease below the viscosity interface (Fig. 4*a*), yielding an effective cessation of seismicity even though the slab continues to descend (Fig. 4*c*).

The fluid-slab model thus allows for the formation of realistic slab profiles, accounts for the depth variation in seismic focal mechanisms observed in most subduction zones, yields the observed pattern of seismicity rate variation with depth, and suggests a simple explanation for how a slab might penetrate aseismically into the lower mantle.

The model does not explain how slabs may undergo continuous compression at all depths; such a deformation pattern, although not common, has been observed beneath Tonga–Kermadec[14] and may perhaps arise from complications of mantle flow created by complex plate and slab geometries, a possibility our simple two-dimensional experiments cannot address. Moreover, the mechanisms behind deep earthquakes are uncertain, and observed seismicity patterns might reflect depth variations in the pressure, temperature or slab composition required for deep seismicity. In this respect, however, the weak-slab model makes it easier to account for deep earthquakes; rather than requiring that a given earthquake mechanism explain the observed variations in seismicity, we see that any mechanism that correlates seismicity with strain rate may be consistent with observation. The ability to allow simple explanations of major phenomena is the most intriguing aspect of the weak-slab model, and suggests that slabs should be viewed not as strong bodies thrust beneath a trench, but instead as weak fluid sheets flowing down into the Earth's mantle. □

Received 13 August 1992; accepted 11 January 1993.

1. Bevis, M. *Nature* **323,** 52–53 (1986).
2. Fischer, K. & Jordan, T. H. *J. geophys. Res.* **96,** 14429–14444 (1991).
3. Giardini, D. & Woodhouse, J. H. *Nature* **307,** 505–509 (1984).
4. Giardini, D. & Woodhouse, J. H. *Nature* **319,** 551–555 (1986).
5. Tao, W. & O'Connell, R. J. *J. geophys. Res.* **97,** 8877–8904 (1992).
6. Gurnis, M. & Hager, B. H. *Nature* **335,** 317–321 (1988).
7. Kincaid, C. & Olson, P. *J. geophys. Res.* **92,** 13832–13840 (1987).
8. Vassiliou, M. S., Hager, B. H. & Raefsky, A. A. *J. Geodyn.* **1,** 11–28 (1984).
9. Ogawa, M. *J. geophys. Res.* **92,** 13801–13810 (1987).
10. Hobbs, B. E. & Ord, A. *J. geophys. Res.* **93,** 10521–10540 (1988).
11. Green II, H. W., Young, T. E., Walker, D. & Scholz, C. H. *Nature* **348,** 720–722 (1990).
12. Kirby, S. H. *J. geophys. Res.* **92,** 13789–13800 (1987).
13. Meade, C. & Jeanloz, R. *Science* **252,** 68–72 (1991).
14. Apperson, K. D. & Frohlich, C. *J. geophys. Res.* **92,** 13821–13831 (1987).
15. Isacks, B. & Molnar, P. *Nature* **223,** 1121–1124 (1969).
16. Isacks, B. & Molnar, P. *Rev. Geophys. Space Phys.* **9,** 103–174 (1971).
17. Creager, K. C. & Jordan, T. H. *J. geophys. Res.* **91,** 3573–3589 (1986).
18. Gable, C. W., O'Connell, R. J. & Travis, B. J. *J. geophys. Res.* **96,** 8391–8405 (1991).
19. Hager, B. H. & O'Connell, R. J. *J. geophys. Res.* **86,** 4843–4867 (1981).
20. Ricard, Y. & Vigny, C. *J. geophys. Res.* **94,** 17543–17559 (1981).

ACKNOWLEDGEMENTS. Supported by the NSF and NASA. We thank the Department of Geology and Geophysics at Princeton University for the use of computer facilities.

Aerodynamics and the evolution of long tails in birds

Andrew Balmford*, Adrian L. R. Thomas & Ian L. Jones*

Department of Zoology, University of Cambridge, Downing Street, Cambridge CB2 3EJ, UK

TWO problems limit the interpretation of recent experiments[1–3] supporting Darwin's[4] suggestion that female choice for ornate males may account for the evolution of long tails in birds. First, in some species tail elongation may have been favoured by natural rather than sexual selection. Second, it is unclear how female preferences for elaborate males have evolved, because current tests of competing models are often inconclusive[5–7]. We have integrated aerodynamics theory with comparative data on sexual dimorphism in tail length to evaluate the flight costs of different forms of tail elongation. We report here that long tails with shallow forks are aerodynamically optimal, exhibit correspondingly low sexual dimorphism and may therefore have evolved under natural selection. Other long-tail types impair flight and show greater sexual

* Present addresses: Institute of Zoology, Zoological Society of London, Regent's Park, London NW1 4RY, UK (A.B.); Department of Zoology, University of British Columbia, 6270 University Boulevard, Vancouver, British Columbia V6T 2A9, Canada (I.L.J.).

dimorphism, but variation in their initial evolutionary cost suggests differences in how female preferences for them may have evolved.

Although evidence is accumulating that in a number of birds females prefer long-tailed mates[1-3], the role of natural selection in tail elaboration has been largely ignored. Evidence that long tails impose viability costs is very limited[8-10], yet without this it remains possible that tail elongation has sometimes been driven by natural selection, perhaps because it improves aerodynamic efficiency, manoeuvrability or stability[11]. Moreover, even where it has been demonstrated that long tails are costly but are preferred by choosy females, resolving how such preferences have evolved is difficult, particularly if females gain no direct benefits from their choice of mating partners[5]. For example, evidence that preferred traits are costly, that they reveal heritable variation in male quality and that discriminating females thereby produce high viability offspring, would be consistent with 'good genes' models of sexual selection[12]. But such results could also be accommodated entirely by Fisherian models[5-7], in which initially arbitrary male traits become increasingly elaborate and costly as a result of coevolution with female preferences for them[13]. An unexplored way to distinguish these competing models may be to switch from examining the contemporary costs of male traits and the benefits of female preferences for them, and to consider instead the costliness of traits during the initial stages of their evolution. Modern Fisherian models make no firm predictions because runaway evolution can occur whether preferred traits are initially costly, beneficial or neutral with respect to natural selection[13]. In contrast, good genes models require that if their evolution is gradual, preferred characters must incur substantial costs even in their simplest form to evolve as reliable indicators of male viability.

We have used a combination of aerodynamic models and comparative data from more than 600 museum skins to examine the costs of tail elongation in birds. Our analysis is based on a new lifting surface model[14] which applies the classical aerodynamic solution of the forces acting on a low aspect ratio delta wing[15,16] to assess the lift and drag associated with a bird's tail. Tails generate lift in proportion to the square of their maximum continuous span. Any area distal to the point of maximum width contributes only drag, which is proportional to total tail area[14]. The aerodynamically optimal tail is therefore triangular when spread, and forked when closed. We examined the aerodynamic implications of different types of tail elongation by modelling progressive elaboration from a short, simple tail in which all feathers are of equal length (see Fig. 1).

Long, graduated tails, in which all but the outermost feathers are elongated, generate the same lift as normal tails (because maximum span is set by the outermost feathers and so does not change) but substantially more drag, as elongation adds considerably to tail area. The aerodynamic cost of the tail (measured here as drag/lift at a constant angle of attack, though other indices give qualitatively similar results) therefore rises sharply with increased length (Fig. 1). In pintails only the central tail feathers are elongated, so that although lift again fails to increase with length, tail area and thus drag rise only slowly. The marginal aerodynamic costs of tail elongation (that is costs per unit length) are therefore relatively slight for pintails. Lastly, if tails become forked (when closed) through elongation of their outer feathers, lift initially increases more rapidly than drag (as the spread tail tends toward the optimum triangular shape), so that aerodynamic costs are lower for long shallow forks than for simple tails[14]. Costs remain essentially unchanged if these forks continue to elongate isometrically, but if elongation instead proceeds by further deepening of the fork through lengthening its outer but not its central feathers, these outer feathers eventually project beyond the point of maximum continuous width even when spread. Drag (but not lift) then increases with length, so that aerodynamic costs rise, albeit at the same low rate as for pintails. Note that use of a more detailed analytical method such as curved lifting line theory[17-19] generates qualitatively similar conclusions to those of our simple general lifting surface approach[14].

TABLE 1 Comparisons of tail length in closely related pairs of long-tailed species

(*a*) Forked versus other tail types

Species pair	Tail shape	Relative tail length: Male	Female	Male:Female
Sterna paradisaea	Fork	1.14	1.04	1.10
Stercocarius longicaudus	Pin	1.37	1.34	1.02
Eupetomena macroura	Fork	1.84	1.73	1.06
Phaethornis superciliosus	Pin	1.52	1.44	1.06
Merops hirundineus	Fork	1.24	1.24	1.00
Merops superciliosus	Pin	1.16	1.11	1.05
Coracias abyssinica	Fork	2.01	1.81	1.11
*Uratelornis chimaera**	Graduated	2.35	1.77	1.33
Gubernetes yetapa	Fork	2.63	2.34	1.12
Alecturus risorius	Pin	2.55	1.59	1.60
Phibalura flavirostris	Fork	1.30	1.17	1.11
Illicura militaris	Pin	1.06	0.69	1.54
Motacilla clara	Fork	1.22	1.30	0.94
Euplectes macrourus	Graduated	1.30	0.62	2.10
Enicurus immaculatus	Fork	1.54	1.54	1.00
Copsychus malabaricus	Graduated	2.10	1.59	1.32
Dicrurus macrocercus	Fork	1.58	1.47	1.07
Elminia longicauda	Graduated	1.93	1.71	1.13

(*b*) Shallower versus deeper forks

Species pair	Male fork depth	Relative tail length: Male	Female	Male:female
Chelictinia ricourii	1.93	1.57	1.48	1.06
Elanoides forficatus	2.53	1.56	1.45	1.08
Sterna melanogaster	2.23	1.23	1.30	0.95
Sterna paradisaea	2.54	1.14	1.04	1.10
Hemiprocne comata	1.92	1.22	1.27	0.96
Hemiprocne longipennis	2.20	1.21	1.01	1.20
Polyonymus caroli†	1.37	1.32	1.14	1.16
Sappho sparganura	2.95	1.99	1.15	1.73
Coracias caudata	1.64	1.34	1.26	1.06
Coracias abyssinica	1.95	2.01	1.81	1.11
Muscipipra vetula	1.45	1.49	1.44	1.03
Gubernetes yetapa	3.62	2.63	2.34	1.13
Hirundo rustica	2.27	1.30	1.21	1.07
Hirundo smithii	2.44	1.19	0.79	1.51
Dicrurus caerulescens	1.30	1.38	1.42	0.97
Dicrurus macrocercus	1.55	1.58	1.47	1.07

All pairs are from the same family or superfamily[21,22] and are roughly matched for size and relative tail length of males, but have otherwise been selected at random. Body length and the lengths of the longest and shortest tail feathers were measured on 10 male and 10 female skins in breeding plumage (except* = only 5 males and 6 females; † = only 8 females). To account for overall size differences between specimens, relative tail length (mean length of left and right longest tail feathers/body length) was calculated, and the ratio of the mean relative tail length of males to that of females then used as an index of sexual dimorphism in tail length. For forked tails, depth is the ratio of the mean lengths of their longest and shortest feathers. In these and all other analyses, we have excluded all species whose long tails may have mechanical functions other than flight (such as acting as a brace when climbing).

This analysis yields a number of testable results. It suggests that, depending on their depth (longest:shortest tail feather length) and how widely they are spread during use, long forked tails may be aerodynamically beneficial and so (unlike other long tails) may have evolved through natural rather than sexual selection. Given that sexual selection in birds usually acts more strongly on males than females[4], we predict that the reduced role of sexual selection in the evolution of long forked tails should mean that these generally exhibit lower sexual dimorphism in length than do long graduated tails or pintails. We tested this by measuring museum skins to compare tail dimorphism (male:female tail length, standardized to body length) in pairs of closely related, long-tailed species, which differed in the shape of their long tails but in few other potentially confounding variables. The results of this pairwise comparative approach[20]

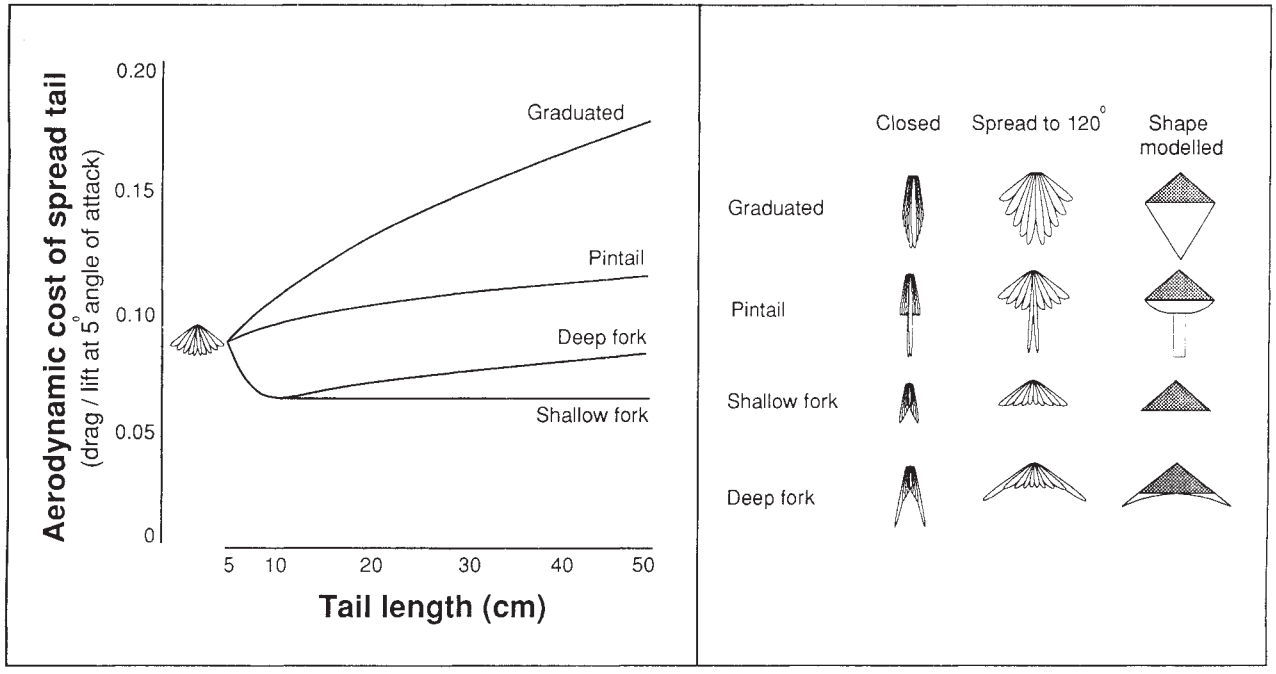

FIG. 1 Aerodynamic costs associated with the progressive elongation of different types of long tails from a simple tail with all feathers 5 cm long. Lift and drag have been calculated for tails spread to an apical angle of 120°. The tail shapes considered are shown in the right-hand panel, together with the corresponding geometric polygons used in the model; stippling indicates what part of each tail generates lift. The marginal costs of elongation of pintails and deep forks will depend only on the width of their streamers, but will always be substantially lower than those of graduated tails, in which nearly all tail feathers are elongated. Tails are assumed to act as stiff flat plates with continuous surfaces[14]. Aerodynamic costs are expressed as the ratio of drag/lift at 5° angle of attack and 5 m s^{-1} freestream velocity. The airflow over the tail is assumed to be a steady uniform flow comprising the vector sum of the bird's velocity and the induced velocity generated by the wings. Flight is assumed to be either normal forward flapping flight[23,24], or gliding[25]. Conclusions are nevertheless robust across a broad array of flight speeds and flow conditions and are unaffected by the precise details of the tail shapes considered.

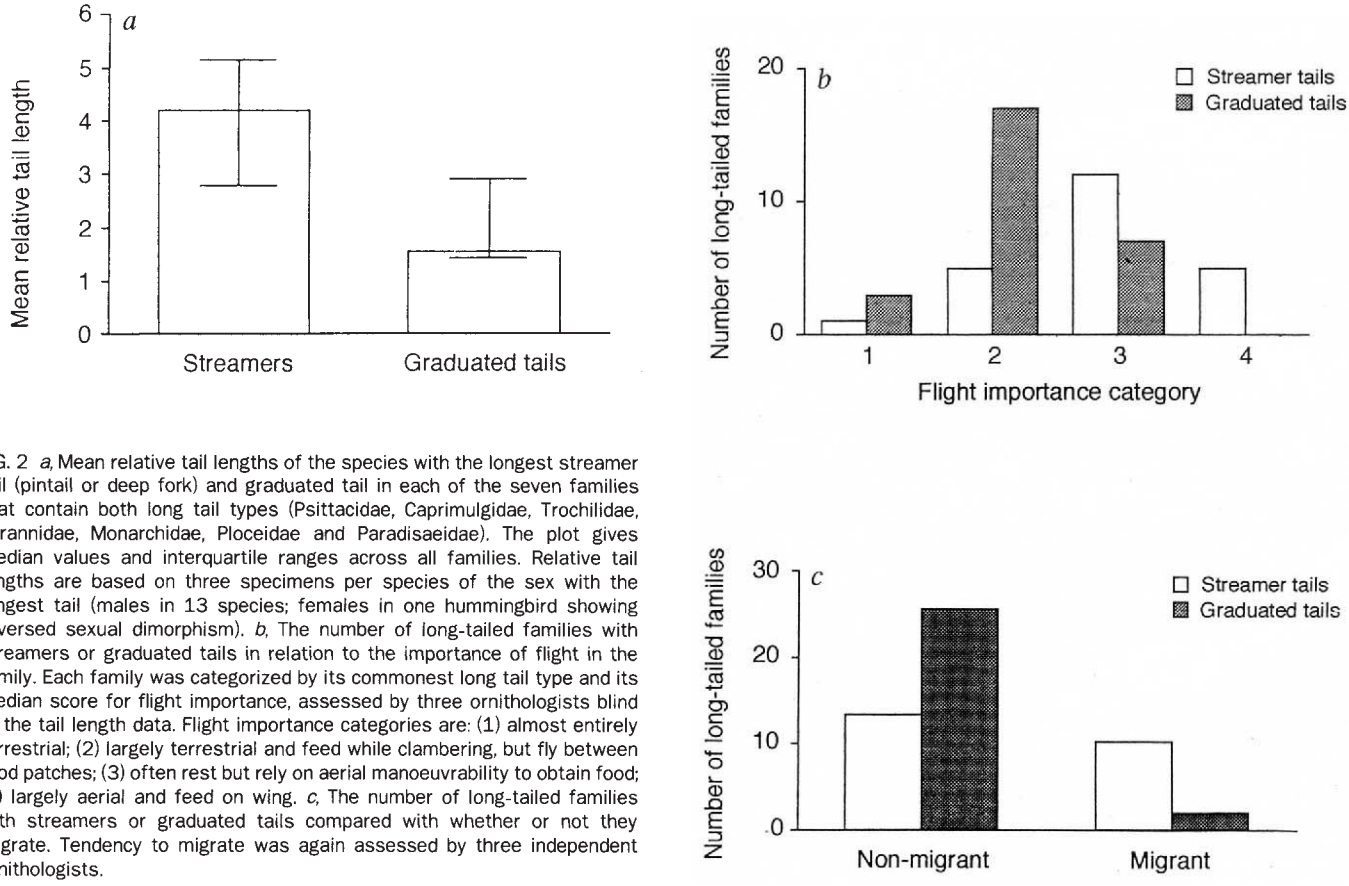

FIG. 2 *a*, Mean relative tail lengths of the species with the longest streamer tail (pintail or deep fork) and graduated tail in each of the seven families that contain both long tail types (Psittacidae, Caprimulgidae, Trochilidae, Tyrannidae, Monarchidae, Ploceidae and Paradisaeidae). The plot gives median values and interquartile ranges across all families. Relative tail lengths are based on three specimens per species of the sex with the longest tail (males in 13 species; females in one hummingbird showing reversed sexual dimorphism). *b*, The number of long-tailed families with streamers or graduated tails in relation to the importance of flight in the family. Each family was categorized by its commonest long tail type and its median score for flight importance, assessed by three ornithologists blind to the tail length data. Flight importance categories are: (1) almost entirely terrestrial; (2) largely terrestrial and feed while clambering, but fly between food patches; (3) often rest but rely on aerial manoeuvrability to obtain food; (4) largely aerial and feed on wing. *c*, The number of long-tailed families with streamers or graduated tails compared with whether or not they migrate. Tendency to migrate was again assessed by three independent ornithologists.

confirm our prediction (Table 1*a*): across nine species pairs, forked tails do indeed show less sexual dimorphism in length than do other long tails (Wilcoxon signed ranks test: $z_{corr} = 2.10$, 1-tailed $P = 0.017$).

Our model also suggests that as long forked tails deepen, it becomes more likely that they are aerodynamically costly (compared with shallow forked tails; see Fig. 1), and therefore increasingly probable that sexual rather than natural selection explains their evolution. If this is so, then among species with long forked tails, sexual dimorphism in tail length should increase with fork depth. Pairwise comparisons of closely related species support this prediction (Table 1*b*). Even where differences in fork depth are slight, these are consistently associated with greater sexual dimorphism in the tails of more deeply forked species (Wilcoxon test across $N = 8$ family pairs: $z_{corr} = 2.52$, 1-tailed $P = 0.006$).

Among those elongated tails that are apparently sexually selected, the marginal costs of graduated tails greatly exceed those of streamer-shaped tails (that is pintails and deep forks; Fig. 1). This generates several predictions. Within families, the lower costs per unit length of streamer tails should mean that they have evolved to a greater maximum length than more expensive, graduated tails. This is indeed the case (Fig. 2*a*): in all seven families with both long-tail types, the maximum length of streamer tails (relative to body length) exceeds that of graduated tails (Wilcoxon test: $z = 2.37$, 1-tailed $P = 0.009$). The last two predictions deal with differences between bird families in their reliance on flight, and therefore in the likely fitness consequences of increased aerodynamic costs. Comparing long-tailed families, as birds spend more time flying and rely more on aerial agility when feeding, we should expect graduated tails to become less common than streamers. Similarly, costlier graduated tails should be less prevalent in families that migrate than in other families. Both of these predictions are confirmed across 50 long-tailed families, categorized according to 'flight importance' and tendency to migrate by three independent ornithologists (Fig. 2*b*, *c*). Families that spend a substantial proportion of time flying and/or feed aerially (flight importance categories 3 and 4) are far less likely to exhibit graduated tails than are more terrestrial families (categories 1 and 2; $\chi^2 = 11.46$, d.f. = 1, $P < 0.001$; Fig. 2*b*). Likewise, where long-tailed birds migrate, they are more likely to possess streamer-shaped tails than are non-migrant birds ($\chi^2 = 8.86$, d.f. = 1, $P < 0.01$; Fig. 2*c*).

Each of the predictions of our aerodynamic analysis is therefore supported by the comparative data, enabling us to make two suggestions about the selective pressures driving tail elongation in birds. First, the theoretical and morphological evidence indicates that while most other types of long tails have probably evolved through sexual selection, natural selection for aerodynamic efficiency may be a sufficient explanation for the evolution of many elongated forked tails. Second, the marginal costs associated with pintails and deep forks are far lower than those of graduated tails. Clearly, even short-tail streamers might represent considerable handicaps in families where the fitness consequences of impaired flight are extremely high. But in other families where flight is less important and both streamers and graduated tails have evolved, our analysis suggests that during their initial evolution, streamers would have been relatively poor indicators of male quality. Thus Fisherian models could account for their initial elaboration, but good genes models probably could not. In contrast, graduated tails would have constituted uncheatable handicaps even in their simplest form, and so are more likely to have evolved as reliable indicators of the viability of potential mates. □

Received 21 October; accepted 31 December 1992.

1. Andersson, M. *Nature* **299,** 818–820 (1982).
2. Møller, A. P. *Nature* **332,** 640–642 (1988).
3. Andersson, S. *Anim. Behav.* **43,** 379–388 (1992).
4. Darwin, C. *The Descent of Man, and Selection in Relation to Sex* (Murray, London, 1871).
5. Kirkpatrick, M. & Ryan, M. J. *Nature* **350,** 33–38 (1991).
6. Balmford, A. & Read, A. F. *Trends Ecol. Evol.* **6,** 274–276 (1991).
7. Jones, I. L. *Auk* **109,** 197–199 (1992).
8. Møller, A. P. *Nature* **339,** 132–135 (1989).
9. Evans, M. R. & Hatchwell, B. J. *Behav. Ecol. Sociobiol.* **29,** 421–427 (1992).
10. Evans, M. R. & Thomas, A. L. R. *Anim. Behav.* **43,** 337–347 (1992).
11. Maynard Smith, J. *Evolution* **6,** 127–129 (1952).
12. Heisler, L. in *Sexual Selection: Testing the Alternatives* (eds Bradbury, J. W. & Andersson, M.) 96–118 (Wiley, Chichester, 1987)
13. Lande, R. *Proc. natn. Acad. Sci. U.S.A.* **78,** 3721–3725 (1981).
14. Thomas, A. L. R. *Phil. Trans. R. Soc.* (in the press).
15. Jones, R. T. National Advisory Committee for Aeronautics, Technical Report **835,** (1946).
16. Jones, R. T. *Wing Theory* (Princeton Univ. Press, Princeton, 1990).
17. Guermond, J. L. *J. Fluid Mech.* **211,** 497–513 (1990).
18. Cheng, H. K. & Murillo, L. E. *J. Fluid Mech.* **143,** 327–350 (1984).
19. van Dam, C. P. *Nature* **325,** 435–437 (1987).
20. Felsenstein, J. *Am. Nat.* **125,** 1–15 (1985).
21. Sibley, C. G., Alhquist, J. E. & Monroe, B. L. Jr *Auk* **105,** 409–423 (1988).
22. Howard, R. & Moore, A. *A Complete Checklist of the Birds of the World* 2nd edn (Academic, London, 1991).
23. Rayner, J. M. V., Jones, G. & Thomas, A. L. R. *Nature* **321,** 162–164 (1986).
24. Spedding, G. R. *J. exp. Biol.* **127,** 59–78 (1987).
25. Spedding, G. R. *J. exp. Biol.* **127,** 45–57 (1987).

ACKNOWLEDGEMENTS. A.B. and A.L.R.T. contributed equally to this work. We thank the staff of the Natural History Museum, Tring, the University Museum of Zoology, Cambridge, and the American Museum of Natural History in New York for access to their collections; M. de L. Brooke, W. Duckworth and M. Evans for scoring flight behaviour; S. Blakeman and A. Willmott for help with measurements; and M. de L. Brooke, N. Davies, C. Ellington, D. Harper, P. Harvey, K. McComb, A. Read and A. Willmott for helpful comments. A.P.B. was supported by Girton College, Cambridge, A.L.R.T. by SERC, and I.L.J. by NSERC, Canada.

Landmark stability is a prerequisite for spatial but not discrimination learning

R. Biegler & R. G. M. Morris*

Laboratory for Neuroscience, Department of Pharmacology, University of Edinburgh Medical School, 1 George Square, Edinburgh EH8 9JZ, UK

NEURONS sensitive to both place and direction from distinct regions of the hippocampal formation[1,2], allometric relationships between spatial learning and hippocampal structure[3,4] and pronounced impairments in spatial learning after lesions in this area[5–8], indicate that the hippocampal formation subserves allocentric spatial learning[9,10]. To learn more about the process of spatial representation, we have developed a task that provides independent control of both landmark and directional cues. On the basis of physiological[11] and behavioural[12] work, this task also makes it possible to investigate the relevance of associative learning principles, such as predictability[13], to the spatial domain. We report here that although rats learn to discriminate between landmarks on the basis of their proximity to a reliably predicted food reward, they will only learn to use them to represent its location if they maintain stable locations within a geometric frame of reference.

We trained 14 male Lister-hooded rats to find food reward in a large directionally polarized arena (Fig. 1*a*). Two landmarks (L+, L−) were arranged to predict the spatial location of hidden food nearby that was either accessible (F+) or inaccessible (F−). The single parameter that we manipulated was whether the landmarks and feeders occupied fixed locations across trials (group fixed) or were moved randomly from trial to trial (group varied). Importantly, when the landmarks were moved between locations, the feeders were also moved such that the spatial relationship between L+ and F+, and between L− and F−, was always maintained; that is, if F+ was 40 cm to the 'south' of L+ for a given rat, it remained so on all trials.

Spatial theories predict that, because only group fixed has the potential of forming a stable geometric representation of the landmarks (that is, 'map'), only they will learn to search at the F+ location. Conversely, application of the associative learning principle of predictability to the spatial domain suggests that both groups should be able to learn to search at F+, but

* To whom correspondence should be addressed.